Study of forming of gradient structure and properties for low-carbon steel in drawing operation with wall thinning

A. I. Olekhver, *Cand. Eng., Associate Prof., E4 "High-Energy Devices of Automatic Systems" Dept.* [1], *e-mail: leshicher@mail.ru;*
E. Yu. Remshev, *Dr. Eng., Associate Prof., Head of the A2 "Technology of Structural Materials and Production of Rocket and Space Technology" Dept.* [1], *e-mail: remshev@mail.ru;*
P. M. Vinnik, *Dr. Eng., Head of the O4 Dept. of Higher Mathematics* [1], *e-mail: vinnik_pm@voenmeh.ru;*
G. A. Vorobyeva, *Cand. Eng., Associate Prof., A2 "Technology of Structural Materials and Production of Rocket and Space Technology" Dept.* [1], *e-mail: vorobeva_ga@voenmeh.ru;*
Z. N. Rasulov, *Cand. Eng., Associate Prof., E4 "High-Energy Devices of Automatic Systems" Dept.* [1], *e-mail: takaevz@mail.ru*

[1] *Baltic State Technical University "VOENMEKH" named after D. F. Ustinov (St. Petersburg, Russia)*

The paper presents the results of experimental examination of material deformed state in the process of realization of its mechanical processing (drawing with thinning). In particular, the new effect were revealed, which were not presented before in the literature; these effects have influence on final deformation forming, especially in the process dynamics. The results of evolution of the material mechanical properties in various cross-sections of semiproducts are presented, accompanied with assessment of their heterogeneity, of microstructure and chemical composition of the alloy after plastic deformation. The ways of further development of researched effects and the factors determining these effects (such as friction and work tool geometry) are suggested.
Key words: mechanics, destruction, material particle, deformation, monotonicity, drawing with thinning, experiment, grade grid, microstructure.
DOI: 10.17580/cisisr.2026.01.10

Introduction

Functional-gradient materials (FGM) are identified as the innovative class of materials with variation of structure, mechanical properties and chemical composition through material depth. Reveal of regularities of varying chemical and physical-mechanical properties in dependence of a distance from separation boundaries of various types allowed to substantiate necessity of introduction of the term "gradient structures" for more wide determination of the material state. Thus, an increasing interest to materials not only with gradient structure but also with a gradient of chemical and physical-mechanical properties is quite correct [1].

The main methods of obtaining the functional-gradient materials on metallic base are determined via the method (route) of technological processing of materials, which are used for their fabrication at the stage of non-uniform structure forming (gradation).

One of the directions of FGM manufacture is use of intensive plastic deformation (IPD) for obtaining a fine-grained material structure, what leads to qualitative variation of material properties. The following conclusions were revealed on the base of publications of well-known national specialists in this area (R. Z. Valiev [2–4] and G. A. Salishchev [5–7]):

1. Cold deformation provides substantial effect on material structure fragmentation.

2. Low-alloy structural not-ageing steels are not considered in the researches, unlike low-carbon high-alloy steels [8–11].

3. Drawing with wall thinness is not examined in the researches [5–7] as potential IPD operations; however, "rolling" of sheet semiproduct demonstrates good results in structure fragmentation and material strengthening.

Experimental methods for determination of the stress-strain state of a billet in the process of drawing with wall thinning were substantiated and developed under leadership of I. P. Renne [12] in Tula mechanical institute (at present time – Tula State University). These methods were also presented and discussed in the work [13]. The problems of analytical calculation of the stress-strain state of a billet, of deformation force, of choosing an optimal technological parameters in the process of drawing with wall thinning were examined (among other problems) in the works of M. V. Storozhev and E. A. Popov [10], A. L. Vorontsov [14].

Anisotropy account of the properties in the process of drawing with wall thinning was examined in the researches at Tula State University, implemented by V. V. Gryazev [15] and S. N. Larin [16], as well as at Samara National Research University named after S. P. Korolev. High results were

achieved in material structure management and optimization of technological processes for manufacturing shell products. However, owing to the features of the aircraft industry, these researches were aimed on aluminium alloys, and technological processes in this industry don't use the process of drawing with wall thinning [17–21].

Drawing with wall thinness is based on significant redistribution of material through its thickness, what is considered as a deformation measure and approximate this processing kind to IPD processes, especially to rolling. However, it requires detailed examination, taking into account stress-strain state of material and rigid scheme of stressed state, which restricts ultimate material ductility.

Thus, generalizing the above-described experience, the aim of this research is the experimental study of forming of gradient structure and mechanical properties of low-carbon steel in the process of drawing with wall thinning and assessment of possibility of its consideration as the IPD process.

Materials and methods

The studies were carried out via the method of grate grid for cutting of billets maxde of high-quality low-carbon steel 11YuA before drawing with wall thinning. Chemical composition of this steel is presented in the **Table 1**. The initial semiproduct has diameter 107.8 mm with wall thickness in the edge part 7.5 mm, and the final semiproduct has diameter 100 mm with wall thickness in the edge part 3.8 mm. These billets were cut by two halves via laser cutting and rectangular grate grid was applied on the obtained cross-sections. One line family is approximately parallel to external surface of billet wall, while another line family is perpendicular to the first line family, i.e. approximately perpendicular to external surface of billet wall. Then halves of billets were glued and these billets were subjected to drawing with wall thinning.

The process was stopped during drawing and the billet was extracted and separated to two initial halves with grate grid in the following cases:

a) after passing of the bottom section of a billet;

b) after passing of the middle of wall height;

c) after passing of almost whole wall – 90 % of wall height;

d) after complete passing of drawing with wall thinning.

To determine mechanical properties of the material of stamped shell, a test for Vickers hardness using the hardness tester HBRV 187.5 and bending test using the testing machine Shimadzu AGX-100 were carried out. These tests were conducted instead of classic extension test, because the material of stamped shell has not high ductility, while the samples are destructed during preparing operation and there is no possibility to prepare the samples for extension test. The samples for testing were cut off from two semiproducts: before and after the operation of drawing with wall thinness. To assess mechanical properties through the whole billet height, the samples were cut off from its lower, middle and edge parts. In order to determine hardness through the walls of semiproducts from its internal and external sides, material layer with thickness 0.5 mm was removed using a milling machine, and hardness was measured. To identify macro- and microstructure, chemical pickling using Nital reactant in nitric acid solution (33 ml of ethanol + 3 ml of HNO_3) was carried out with holding time 5–10 s. Chemical composition of the surface of samples was examined using the scanning electron microscope Mira Tescan with the system of energy-dispersive microanalysis AztecLive Advanced Ultim Max 65. Analysis of an average grain size was determined in accordance with the GOST 5639-82. Scale 1 Vickers microhardness was determined in accordance with the GOST 9450-76, load during measuring was 500 g and hardness indentation time was 10 s.

Results and discussion

The conducted experiments allowed to reveal the new features of material flow dynamics during drawing with wall thinness, which were not previously reflected in the technical literature and provide substantial input in comprehension of process physics, despite rather small quantitative effect of forming mechanical properties of billet material.

Maximal interest (from the point of view of material deformation kinematics) is focused on a plastic deformation area at the stationary stage of semiproduct drawing (see **Fig. 1**). This picture allows fixing chronological sequence of semiproduct material deformation from the entrance in the main area of plastic deformation to its final forming. The following sequence of forming can be noted:

– inclination of the straight line interval in the direction of work tool motion in the zone adjacent to a plastic deformation area;

– bending in the central part of a line interval with saving straightness of edges in an upper cross-section of a matrix cone part;

– further curve bending in a lower cross-section of a matrix cone part;

– inclination of the straight line interval adjacent to external surface of semiproduct and forming of final fiber form, close to a straight line interval.

Firstly, let us note that the above-mentioned lowering of external edge of cross fiber before the entrance in the plastic deformation area, with absence of such lowering after the plastic deformation area, means that summarized distance between cross fibers along external surface is smaller than along the internal one. Respectively, the external layers should be positioned in compression conditions.

Secondly, it can be concluded from the described kind of form variation for cross fiber during deformation that speed values of motion of material particles of cross fiber vary in the process of passing through the plastic deformation area. The

Table 1. Chemical composition of high-quality low-carbon steel 11YuA

Steel grade	Content, %								
	Carbon	Manganese	Not more than						
			Silicon	Phosphorus	Sulfur	Chromium	Nickel	Copper	Aluminium
11YuA	0.09–0.013	0.3–0.5	0.13	0.025	0.025	0.2	0.15	0.2	0.03–0.09

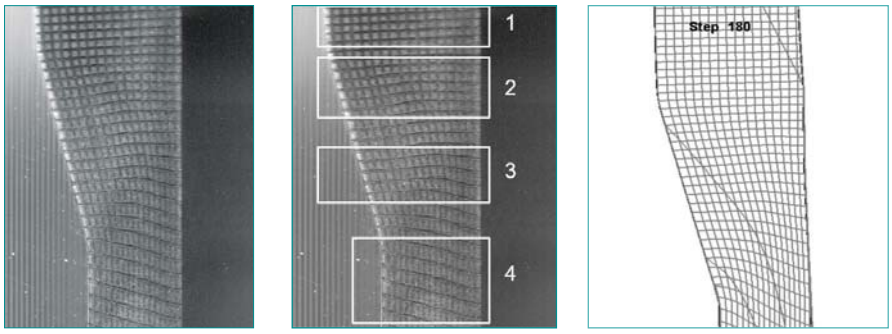

a *b* *c*

Fig. 1. Grate grid in the plastic deformation area:
a) original picture; *b*) deformation stages are underlined; *c*) computer-aided simulation

particles near internal, middle and external surfaces of a product become the most rapid moving particles in this succession.

Thirdly, it is necessary to mention that relative transfer of external edge of cross fiber is at first lower than that of internal edge, and then higher that internal edge. It means that the real trajectory length of metal flow for external layers is larger that it seems to be in the case of typical deformation calculation for relative varying of shape and dimensions of a grate grid cell in comparison with its primary shape and dimensions. This appearance can be explained by bending of cross fiber in the opposite directions. The distance between cross fibers along internal edge differs from the distance along external edge, respectively deletion of cells along internal and external contours is not equal.

All above-described testaments display on the expressed non-monotonicity of drawing process with wall thinness (monotonicity is accepted in determination b y G. A. Smirnov-Alyaev [22, p. 44]. To assess deformation forming for various variants of tool geometry and wear, it is evidently required to apply a computer simulation method. Simulation of the operation was carried out for verification, in accordance to technological features of the experimental research. Fig. 1, *c* displays a grate grid in the plastic deformation area based on the results of experimental research and computer simulation, what confirms definitely adequacy of deformation state calculation using a software package. Two complexes of calculating experiments were conducted with varying (I) the matrix cone angle (evaluating a preliminary inclination angle) and (II) the friction coefficient at the contact surface of a die and punch.

Material deformation process in three cross-sections, which are equally distributed along height of semiproduct generating line, was carried out. This deformation process was conducted with various angles of die slope from 10 to 20 degrees. The obtained results are presented in the **Fig. 2**.

The obtained results allow to make a conclusion that metal flow is less intensive in a bottom and middle casting nozzle cross-section in comparison with a top one; it testifies on low deformation values. It is also concluded that metal in a top cross-section of semiproduct will be characterized by rather higher deformation for large "preliminary inclination angles"; additionally this deformation is alternating. Potentially it can be a cause of material stability loss and can lead to forming of surface and internal defects.

Determination of the deformed state using the grate grid is based on the admission about deformation monotonicity, thereby deformation degree can be set to deformation intensity. To assess the deformed state in this research, the method by P. O. Pashkov was chosen; it is based on acquiring of a parallelogram form by a square cell after deformation. The first and the second deformation components were determined via the formula:

$$e_{1,2} = \frac{1}{2} ln \frac{a_1^2 + b_1^2 \pm \sqrt{\left(a_1^2 + b_1^2\right)^2 - 4a_1^2 b_1^2 sin^2 \delta_1}}{2a_0^2},$$

where a_1 and b_1 are sizes of parallelogram sides after deformation; δ_1 is the angle between parallelogram sides; a_0 is a cell side before deformation, equal to 0.5 mm.

The outline of deformed wall in a lower calculating cross-section after deformation is displayed in the **Fig. 3**.

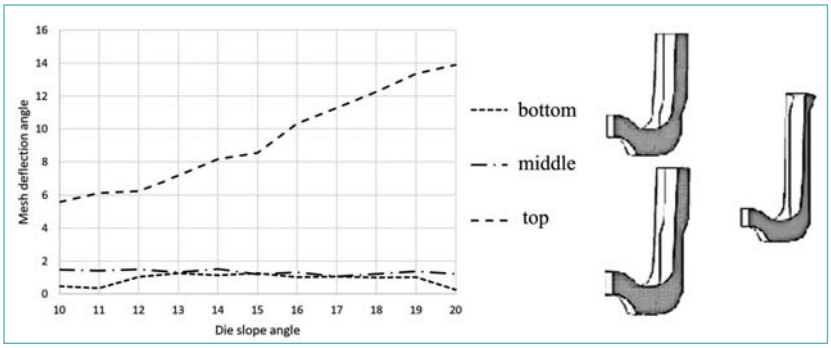

Fig. 2. Relationship between grid inclination angle and die slope angle and outlines of semiproucts at different deformation stages

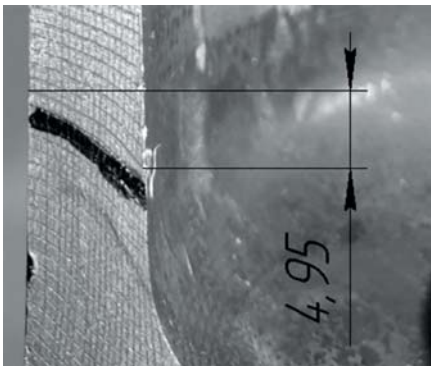

Fig. 3. The outline of deformed wall in a lower cross-section

Deformation intensity is determined according to the following relationship:

$$\varepsilon_i = \frac{\sqrt{2}}{3}\sqrt{(\varepsilon_1-\varepsilon_2)^2+(\varepsilon_2-\varepsilon_3)^2+(\varepsilon_3-\varepsilon_1)^2} \ .$$

The hardness measuring results for samples are shown in the **Fig. 4**. The blue and the red lines display the sample before and after drawing respectively.

Similar to hardness distribution character in the middle cross-section, the edge part is apparently characterized by material strengthening after stamping. Maximal and minimal hardness values for the sample before deformation are equal to 238 HV and 209.8 HV, while maximal and minimal hardness values for the sample after deformation are equal to 285 HV and 226.1 HV. The relationships of deformation intensity and material hardness of semiproduct in control cross-sections, which were obtained experimentally, are displayed in the **Fig. 5**.

Material hardness and deformation degree are distributed in the lower cross-section with non-uniformity 20.6 % and 23 % respectively. It is important that the maximal and minimal values of deformation intensity coincide with the maximal and minimal values of hardness, what corresponds to internal and external surfaces. As for other parts, hardness distribution is non-uniform. Analysis of non-uniform distribution of mechanical properties (see **Table 2)** showed that non-uniformity level in billets before deformation drops with approximation to the edge part of semiproduct. The same tendency is observed for semiproducts after drawing with thinning.

Table 2. Evaluation of distribution non-uniformity for mechanical properties

Sample	K_{HV}, %	K_{ε_i}, %
3.1.1	17.4	–
3.2.1	12.8	–
3.3.1	11.8	–
4.1.1	11.6	17
4.2.1	11.3	26
4.3.1	20.6	23

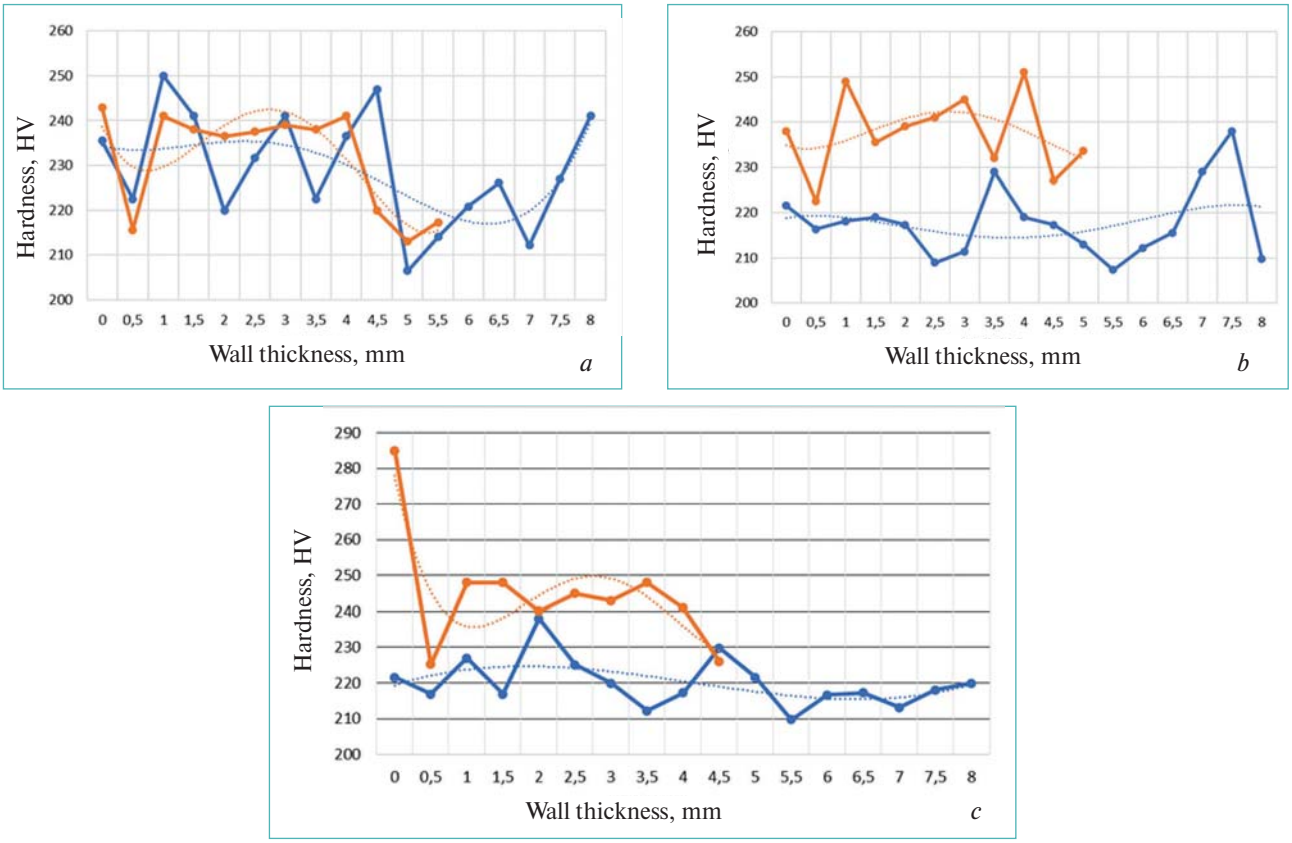

Fig. 4. Hardness distribution along wall thickness or the lower part (*a*), middle cross-section (*b*), edge part of semiproduct (*c*)

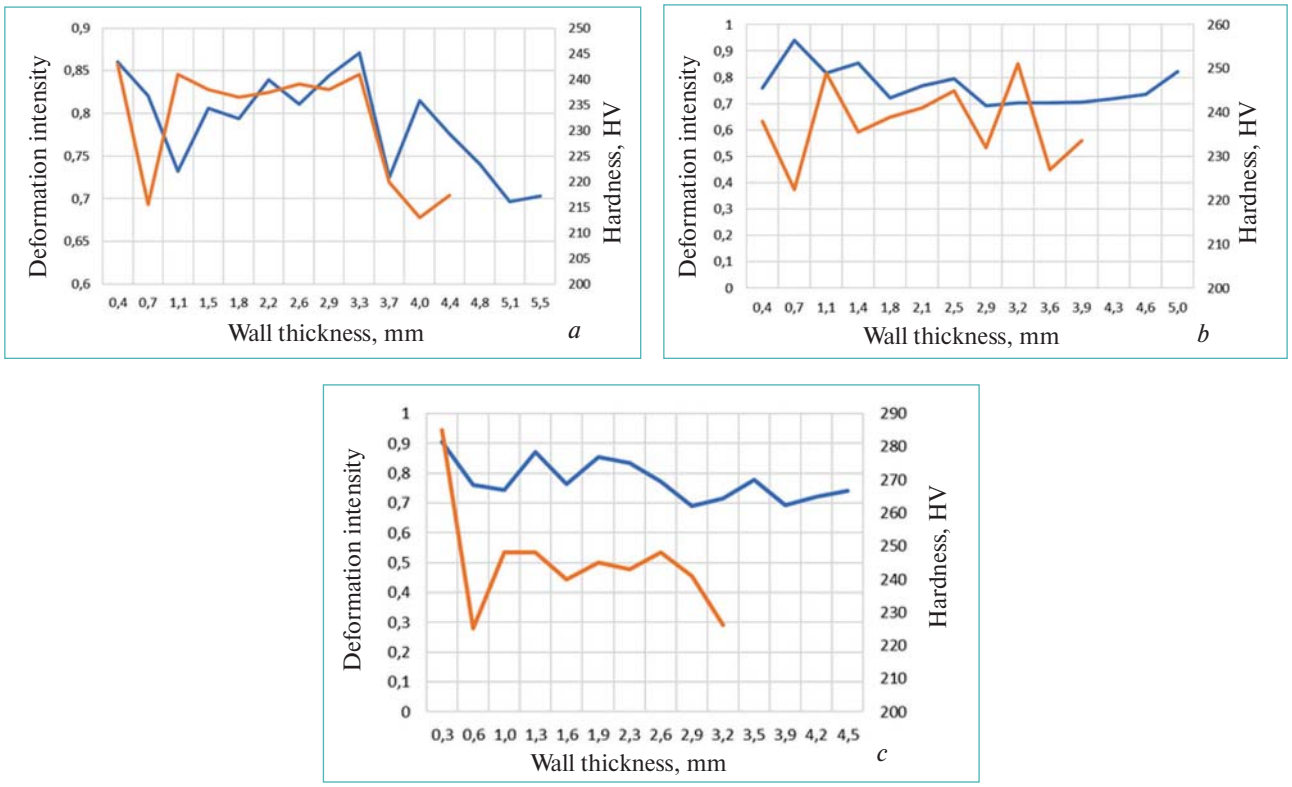

Fig. 5. Distribution of deformation intensity (blue line) and hardness (red line) for the lower part (*a*), middle cross-section (*b*), edge part of semiproduct (*c*)

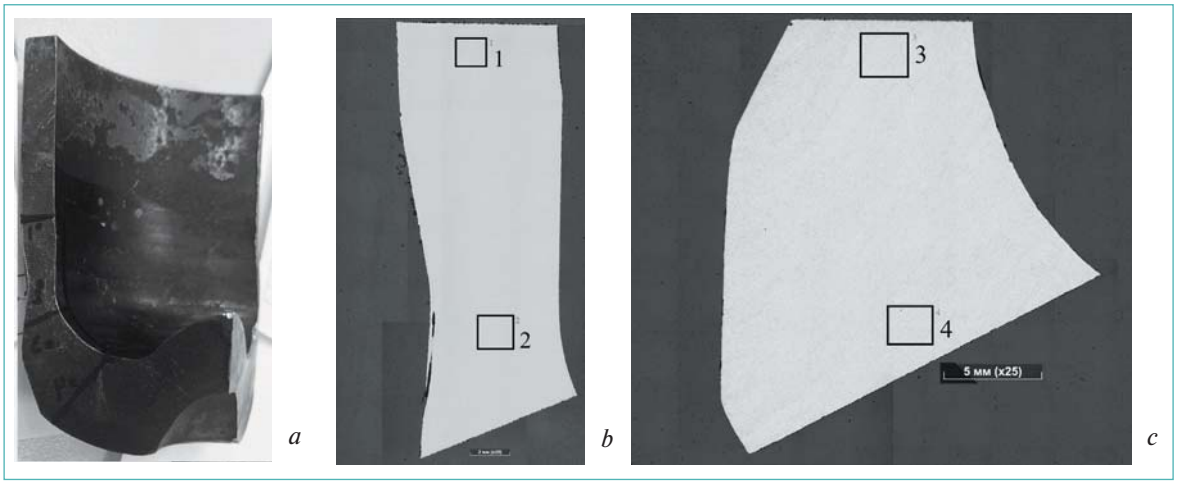

Fig. 6. The scheme of location of cross-sections for microstructural analysis, × 25: general view panorama (*a*), plastic deformation area (*b*), bottom part of semiproduct (*c*)

The definite cross-sections were chosen for conducting metallographic investigations aimed on microstructure evaluation of billets made of 11YuA steel. Location of these cross-sections is displayed in the **Fig. 6**.

The results of macro- and microstructural analysis in the plastic deformation area are presented in the **Fig. 7**.

Microstructure of the examined samples consists of ferrite grains (white areas) and pearlite (dark areas). Pearlite presents a lamellar form. The area 2 (see the Fig. 7, *c* and 7, *d*) is characterized by deformation strengthening of ferrite grains due to plastic deformation. The results of evaluation of structure, average structure of grains and microhardness are presented in the **Table 3**.

Based on the results of microhardness measuring in the zone where plastic deformation didn't occur (areas 1 and 4), microhardness made 108–123HV, and for the areas 2 and 3 it was within the range 185–206HV. Several features can be underlined.

1. The microhardness values in the non-deformed zone of the areas 1 and 4 (ferrite + pearlite structure) after recrystallization annealing before drawing should be similar. However, these values differ substantially (in average

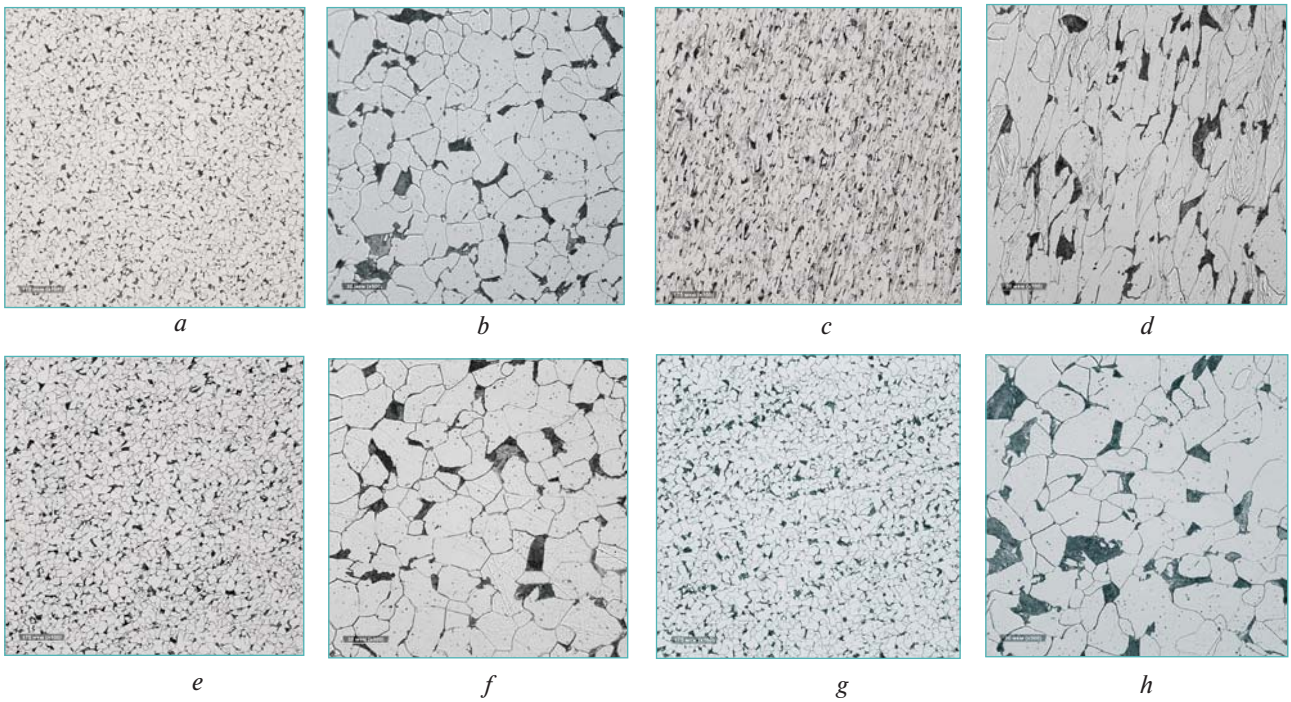

a *b* *c* *d*

e *f* *g* *h*

Fig. 7. Microstructure ×100 (*a*) and x500 (*b*) in the area of the part 1; ×100 (*c*) and ×500 (*d*) in the area of the part 2; ×100 *(e)* and ×500 *(f)* in the area of the part 3; ×100 *(g)* and ×500 (*h*) in the area of the part 4 (in correspondence to the Fig. 6)

Table 3. The results of evaluation of structure, average structure of grains and microhardness

The area (see Fig. 7)	Structure	Grain ball	HV0.5
1	Ferrite + pearlite	9	123 ± 4
2	Ferrite + pearlite	8	206 ± 8
3	Ferrite + pearlite	8	185 ± 12
4	Ferrite + pearlite	8	108 ± 8

by 20 %), what means an influence effect of preliminary plastic deformation in the zone of semiproduct wall, for a stamping operation "folding". Recrystallization annealing evidently does not allow to restore completely material state to initial one.

2. Plastic deformation increases microhardness in average by 2 times (comparison between the areas 2 and 4). The area 3 (corresponding to the Fig. 7 and **Fig. 8**) is not located directly in the plastic deformation area (Fig. 8); structure and grain size are similar to the area 4, however, microhardness slightly (about 10 %) varies from material of the deformed area.

Additional zones in the areas 1–4 (**Fig. 9**) were considered for detailed analysis of microstructure evolution of semiproduct in the examined cross-sections. Microstructure images in the additional zones are presented in the **Fig. 10**.

The area 2 with the sub-areas 2.1–2.3, where 2.1 is adjacent to a die surface and 2.3 is adjacent to a punch surface,

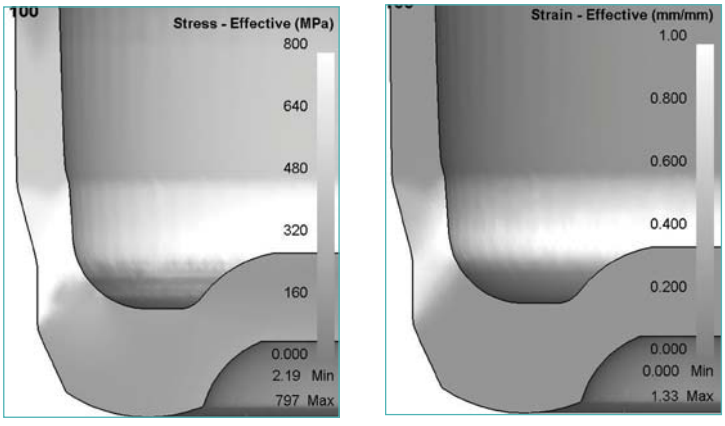

a *b*

Fig. 8. Distribution of stress intensity (*a*) and deformation intensity (*b*) in the plastic deformation area

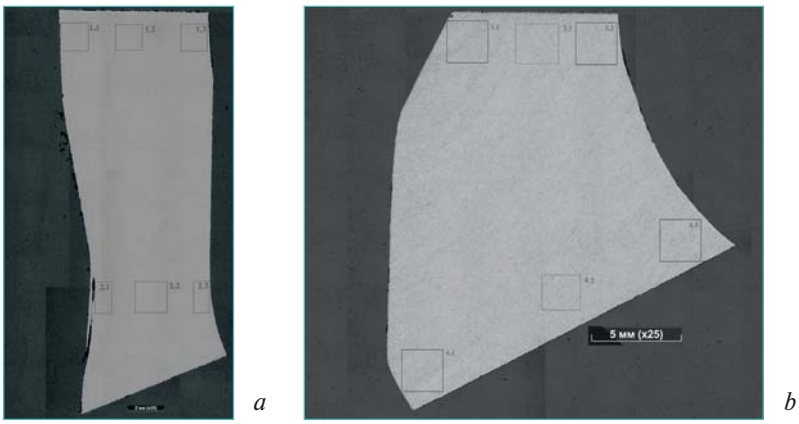

a *b*

Fig. 9. Location of additional zones,×25: general view panorama of in the place of plastic deformation area (*a*) and bottom part of semiproduct (*b*)

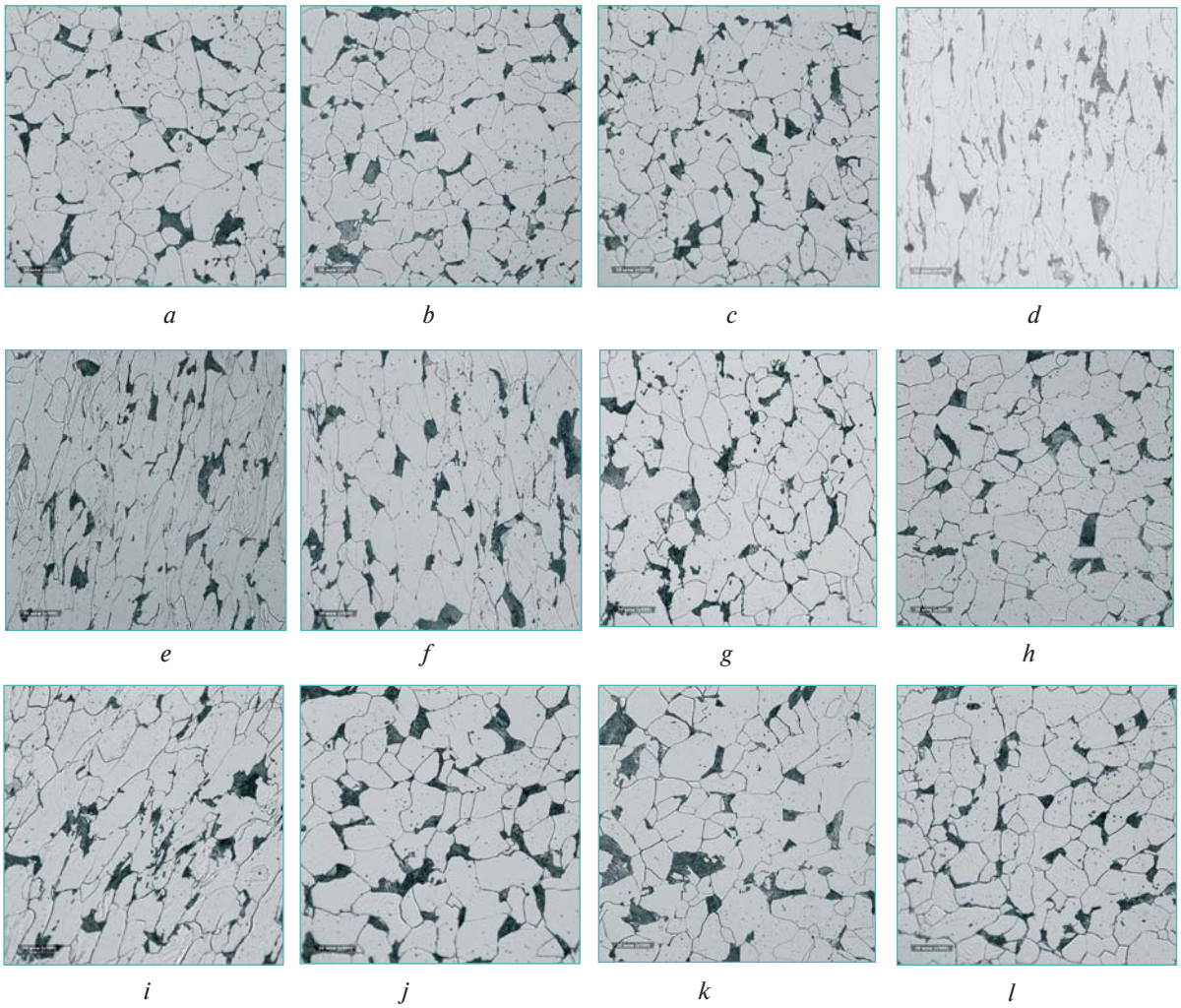

a *b* *c* *d*

e *f* *g* *h*

i *j* *k* *l*

Fig. 10. Microstructure images in the additional zones, ×500 in the zones of he area 1 – 1.1 (*a*), 1.2 (*b*), 1.3 (*c*); **in the zones of he area 2 –** 2.1 (*d*), 2.2 (*e*), 2.3 (*f*)**; in the zones of he area 3 –** 3.1 (*g*), 3.2 (*h*), 3.3 (*i*)**; in the zones of he area 4 –** 4.1 (*j*), 4.2 (*k*), 4.3 (*l*)

causes maximal interest. Pictures of microstructure, which were inverted by colour for simplification of analysis and evaluation, are presented below. As for the area 3, only the sub-area 3.3 has deformed grains with shift stripes, which is explained by its location approximately in one area with the sub-area 2.3.

Grains in the structure of 11YuA steel are distributed in non-uniform mode, their deformation stripes, which are extended along the drawing direction, include ferrite grains with size from 10 μm through 20 μm to 40 μm in transversal direction with essential longitudinal length (up to 90 μm and more) and pearlite grains with size 3–5 μm (in strongly

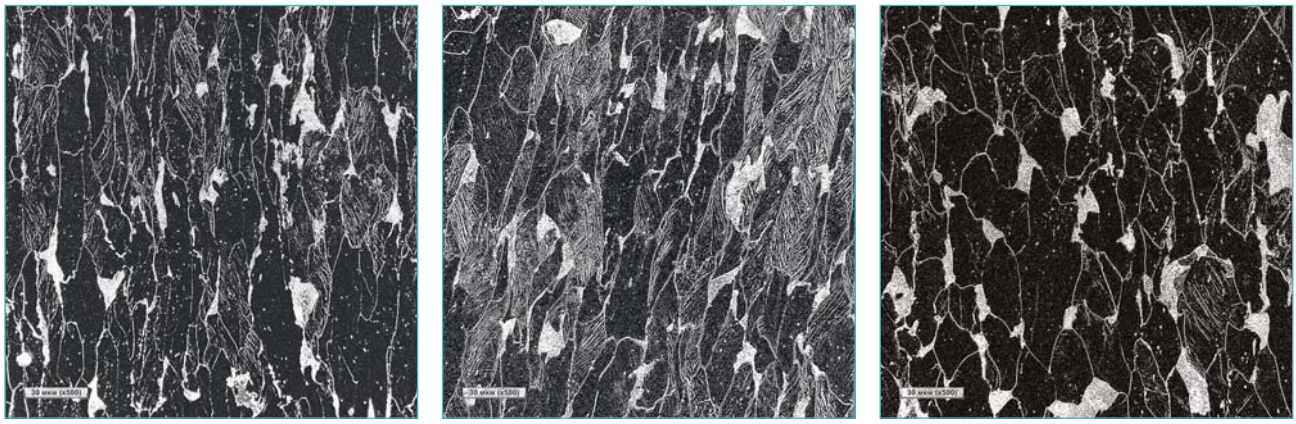

a *b* *c*

Fig. 11. Inverting microstructure image of the sub-areas 2.1 (*a*), 2.2 (*b*) and 2.3 (*c*)

deformed areas) and 15–20 μm (in slightly deformed areas). Separate sections in deformation stripes are slightly mutually disoriented. In strongly deformed areas inside a grain, neighbor sub-grains (blocks) can be turned relatively to each other for substantial number of degrees: structure is characterized by presence of sub-grains with observed shift stripes having different density of their distribution, and by presence of blocks with absence of shift stripes (sub-area 2.1 in the **Fig. 11,** *a*). Grains with absence shift stripes are characterized by increased number if dispersed inclusions.

The sub-area 2.2, which corresponds to wall thickness middle of semiproduct, is deformed intensively during the examined drawing operation. Ferrite grains in deformation stripes have smaller size both in transversal (5–10–30 μm) and in longitudinal (10–30–60 μm) in comparison with deformation stripes of the sub-area 2.1. In this case increased density of shift stripes (the sub-area 2.2, Fig. 11, *b*) and smaller size of sub-grains (3–5–10 μm) is typical for deformed ferrite grains.

The sub-area 2.3 is the smaller deformed one during drawing among examined sub-areas. This steel is characterized by deformation only by single grains with their size corresponding approximately to the size of grains in the sub-area 2.1. Sub-grains with restricted sizes and with shift strips of small distribution density are presented in these deformed grains.

When comparing the obtained results, we can note non-correspondence between quantitative values of deformation intensity (see Fig. 8), where the maximal size corresponds to the surface adjacent to a punch (the sub-area 2.3) and evaluation of deformation level for microstructure varying, where the sub-area 2.3 is characterized by minimal variation of grain forms and sizes.

It should be mentioned especially that the "picture" of deviation of initial grains orientation is rather similar to the data presented for a steel subjected to cold symmetric and asymmetric rolling [3, Fig. 21, *d* and 21, *e*].

Conclusion

It was established experimentally that wall material was subjected to some plastic deformation before entering the plastic deformation area during drawing with wall thinning of the steel 11YuA semiproduct.

This deformation is characterized as differently directional in the edge of a billet wall: at first elongation along the one main axis and shortening along the other main axis occur and then deformation direction changes to the opposite one.

Material tensile strength increases by 20–25 %. Material hardness values before and after operation increases in the central and edge parts of a semiproduct approximately by 20 %. Non-uniformity of material mechanical properties by wall thickness reaches 20 %.

Microstructure of the steel 11YuA after drawing with wall thinning is characterized (in the zone with maximal deformation) by essential disorientation and refinement of grains and blocks, by non-uniform grain deformation along wall thickness in the control cross-sections, as well as by moderate hardness increase by ~ 15–20HV relating to the initial state.

The obtained results confirm that drawing with wall thinning of the steel 11YuA allow to change substantially material structure and its properties in longitudinal and transversal directions and thereby to determine the gradient of material properties.

Further examination of regularities of forming the material structure and properties , technological possibilities of their prediction and determination relating to the tool shape and the conditions of technological operation implementation is considered actual.

The research was carried out under financial support of the RF Ministri of Science and Higher Education (Scientific and research work "Study and prediction of gradient strength fields and plastic parameters of metals in cold metal forming processes with complicated loading", FZWF-2024-0006).

REFERENCES

1. Minko D. V., Belyavin K. E., Sheleg V. K. Theory and practice of obtaining functional and gradient materials via impulse electrophysical methods. Minsk : BNTU, 2020. 450 p.
2. Valiev R., Langdon T. Principles of equal-channel angular pressing as a processing tool for grain refinement. *Progress in Materials Science*. 2006. Vol. 51. pp. 881–891. DOI: 10.1016/j.pmatsci.2006.02.003.
3. Edalati K., Ahmed A., Akrami S., Ameyama K., Aptukov V., Asfandiyarov R., Ashida M., Astanin V., Bachmaier A., Beloshenko V., Bobruk E., Bryła K., Cabrera J., Carvalho A., Choi In-Chul,

Chulist R., Cubero-Sesin J., Davdian G., Zhu Yuntian. Severe plastic deformation for producing superfunctional ultrafine-grained and heterostructured materials: An interdisciplinary review. *Journal of Alloys and Compounds*. 2024. 1002. 174667. DOI: 10.1016/j.jallcom.2024.174667.
4. Valiev R., Alexandrov I., Kawasaki M., Langdon T. Ultrafine-Grained Materials. DOI: 10.1007/978-3-031-31729-3_1.
5. Panov D., Kudryavtsev E., Naumov A., Pertsev A., Simonov Yu., Salishchev G. Evolution of Gradient Structure Under Heat Treatment of Metastable Austenitic Stainless Steel Subjected to Cold Radial Forging. *Metal Science and Heat Treatment*. 2023. Vol. 65. DOI: 10.1007/s11041-023-00963-6.
6. Chernichenko R., Panov D., Naumov S., Kudryavtsev E., Mirontsov V., Salishchev G., Pertsev A. Evolution of the structure, texture and mechanical properties of a cold-swaged austenitic stainless steel during post-deformation annealing. *Fizika metallov i metallovedenie*. 2023. Vol. 124. pp. 524–532. DOI: 10.31857/S0015323023600120.
7. Panov D., Chernichenko R., Naumov S., Pertsev A., Stepanov N., Zherebtsov S., Salishchev G. Excellent strength-toughness synergy in metastable austenitic stainless steel due to gradient structure formation. *Materials Letters*. 2021. 303. 130585. DOI: 10.1016/j.matlet.2021.130585.
8. Sergeev S. N., Safarov I. M., Zhilyaev A. P. et al. Influence of deformation and thermal effect on forming the structure and mechanical properties of low-carbon structural steel. *Fizika metallov i metallovedenie*. 2021. Vol. 122. No. 6. pp. 665–672. DOI: 10.31857/S0015323021060097.
9. Kimura Y., Inoue T. Influence of warm tempforming on microstructure and mechanical properties in an ultrahigh-strength medium-carbon low-alloy steel. *Metallurgical and Materials Transactions A: Physical Metallurgy and Materials Science*. 2013. Vol. 44. No. 1. pp. 560–576. DOI: 10.1007/s11661-012-1391-2.
10. Kryucheva K. D., Putilova E. A., Zadvorkin S. M. et al. Study of structure, microhardness and magnetic parameters of austenitic steel 04Kh17N8T with varying surface strengthening conditions. *Zavodskaya laboratoriya. Diagnostika materialov*. 2025. Vol. 91. No. 3. pp. 42–47. DOI: 10.26896/1028-6861-2025-91-3-42-47.
11. Lobanov M. L., Pyshmintsev I. Yu., Urtsev V. N. et al. Texture heredity in ferrite-martensite structure of a low-alloy steel after controlled thermomechanical treatment. *Fizika metallov i metallovedenie*. 2019. Vol. 120. No. 12. pp. 127–1285. DOI 10.1134/S0015323019120106.
12. Renne I. P., Kuznetsova E. A., Kuznetsov V. P. Heterogeneity of deformations and mechanical properties through wall thickness during drawing with thinning. *Kuznechno-shtampovochnoe proizvodstvo*. 1969. No. 2. pp. 21–25.
13. Smirnov-Alyaev G. A., Chikidovskiy V. P. Experimental studies in metal forming. L. : Mashinostroenie. 1972. 360 p.
14. 14. Storozhev M. V., Popov E. A. The theory of metal forming. M. : Mashinostroenie. 1977. 423 p.
15. Vorontsov A. L. Theory and calculations in metal forming processes. Vol. 2. M. : Izdatelstvo MGTU im. N. E. Baumana. 2014. 441 p.
16. Gryazev M. V., Yakovlev S. S., Pilipenko O. V., Tregubov V. I. Drawing with wall thinning of axial symmetric components made of dual-layered anisotropic materials. *Izvestiya Tulskogo gosudarstvennogo universiteta. Tekhnicheskie nauki*. 2015. No. 1. pp. 3–16.
17. Gryazev M. V., Yakovlev S. S., Travin V. Yu. Experimental studies of the force operating conditions during drawing with wall thinning of axial symmetric components made of dual-layered steel. *Izvestiya Tulskogo gosudarstvennogo universiteta. Tekhnicheskie nauki*. 2015. No. 6-1. pp. 220–223.
18. Larin S. N., Pasynkov A. A., Yakovlev S. S. Assessment of complicated stress state of a billet during drawing through a die with complicated shape. *Izvestiya Tulskogo gosudarstvennogo universiteta. Tekhnicheskie nauki*. 2019. No. 10. pp. 466–470.
19. Aryshenskiy E. V., Aryshenskiy V. Yu., Ragazin A. A. et al. Influence of HF and Er additives on forming of mechanical properties and microstructure in the alloys of Al-Mg-SC-Zr system. *Vestnik Samarskogo universiteta. Aerokosmicheskaya tekhnika, tekhnologii i mashinostroenie*. 2024. Vol. 23. No. 1. pp. 137–146. DOI: 10.18287/2541-7533-2024-23-1-137-146.
20. Erisov Ya. A., Grechnikov F. V., Surudin S. V., Razzhivin V. A. Study f the effect of crystallographic texture on the curves of the ultimate deformations in sheet billets. *Izvestiya Samarskogo nauchnogo tsentra Rossiyskoy akademii nauk*. 2020. Vol. 22. No. 2 (94). pp. 118–123. DOI: 10.37313/1990-5378-2020-22-2-118-123.
21. Erisov Ya., Kuzin A., Sedelnikov A. An Analytical Model for the Plastic Bending of Anisotropic Sheet Materials, Incorporating the Strain-Hardening Effect. *Technologies*. 2024. Vol. 12. No. 12. pp. 236. DOI: 10.3390/technologies12120236.
22. Smirnov-Alyaev G. A. Material resistance to plastic deformation. L. : Mashinostroenie. 1978. p. 368.